Characterizing the hard x-ray diffraction properties of a GaAs linear Bragg–Fresnel lens

Youli Li,[a) Gerard C. L. Wong,[b) Ryan Case, and Cyrus R. Safinya
Materials Research Laboratory, Materials and Physics Departments, University of California, Santa Barbara, California 93106

Ernie Caine and Evelyn Hu
Electrical and Computer Engineering Department and National Nanofabrication Users Network (NNUN), University of California, Santa Barbara, California 93106

Patricia Fernandez
The Advanced Photon Source, Argonne National Laboratory, Argonne, Illinois 60439

We investigated the diffractive focusing properties of (111) GaAs linear Bragg–Fresnel lenses (BFLs) developed for hard x-ray microscopy and microdiffraction of complex materials in confined geometries. We demonstrated that the use of GaAs yields significant processing advantages due to the reduced zone depth. Focal plane diffraction patterns of linear BFLs measured at the advanced photon source using 8–40 keV x rays were compared to a simple model based on Kirchhoff–Fresnel diffraction theory. Good agreement was obtained between experimental data and model calculations using only zones within an effective aperture defined by the transverse coherence of the source. © *2000 American Institute of Physics.* [S0003-6951(00)00929-3]

Diffractive optics in recent years have found increasing use as primary focusing elements in hard x-ray microscopy,[1–3] providing structural and chemical imaging capabilities on submicron to nanometer length scales. The advent of third generation synchrotron sources with high spatial coherence has enabled the effective utilization of transmission Fresnel zone plates and reflective Bragg–Fresnel optics.[4–6] These diffractive lenses are generally three-dimensional structures composed of finite-thickness Fresnel zones. It has been shown that Bragg–Fresnel lenses (BFLs), which are surface relieved Fresnel zones fabricated on single crystal substrates, possess the unique energy-independent focusing capability and are thus advantageous at high energies (>40 keV).[1]

In terms of diffractive properties, a BFL presents an interesting system where dynamical x-ray diffraction by the crystal lattice is coupled with spatial dispersion of the surface Fresnel zones. A number of theoretical models have been proposed for these types of surface-relieved Fresnel structures based on dynamical diffraction theory and quantum scattering theory.[7–9] These models generally are computationally intensive, which hindered direct comparison with experimental data and limited their use in iterative computer aided design of BFLs. We developed a simple model for linear BFLs based on Kirchof–Fresnel diffraction theory assuming a spatially extended, partially coherent source. Model simulations show good agreement with focal plane diffraction patterns measured experimentally at the advanced photon source (APS). This simple model will be useful for design optimization and performance prediction of future lenses.

The BFLs were fabricated using electron beam lithography and reactive ion etching (RIE) methods.[10] The use of GaAs substrates provides an important processing advantage: the zone depth of GaAs BFLs is ~50% of that for Si, which alleviates many feature aspect-ratio (zone width/depth) related processing difficulties. Figure 1 shows a scanning electron microscope (SEM) image of a linear GaAs BFL.

Measurements of the diffractive focusing properties of linear GaAs BFLs were conducted at the Synchrotron Radiation Instrumentation Collaborative Access Team (SRI-CAT) undulator beamline 1-ID-C at the APS in the energy range of 8–40 keV. The experimental setup is schematically shown in Fig. 2 (top). The LN$_2$-cooled double crystal Si (311) monochromator has an energy bandwidth of $\Delta\lambda/\lambda \sim 10^{-5}$, which at 12 keV ($\lambda = 1.032$ Å) gives a longitudinal (temporal) coherence of $\lambda^2/\Delta\lambda \approx 10$ μm. The natural transverse (spatial)
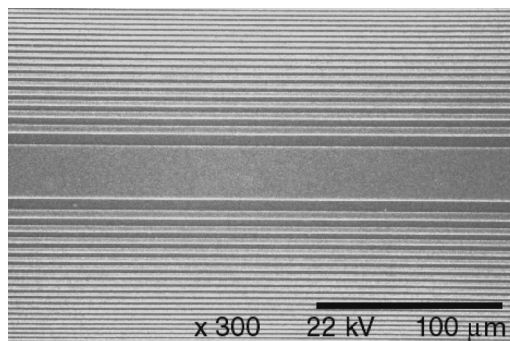

FIG. 1. A scanning electron microscope image of a GaAs linear BFL showing an area near the central zone. The smallest outermost zones produced so far were 0.2 μm. Multiple devices have been stitched together to form long BFLs with zone lengths up to 10 mm.
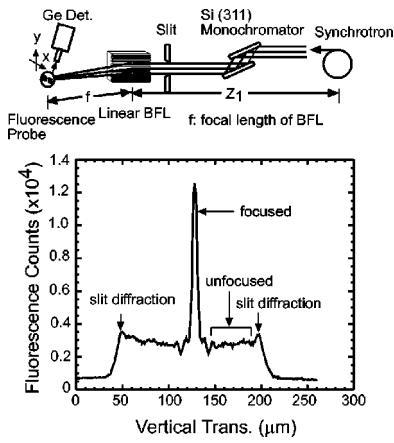
FIG. 2. A schematic drawing of the experimental setup used at the advanced photon source to measure diffraction patterns of linear BFLs (top graph). A typical focal plane diffraction pattern mapped with the fluorescence probe is shown on the bottom graph.
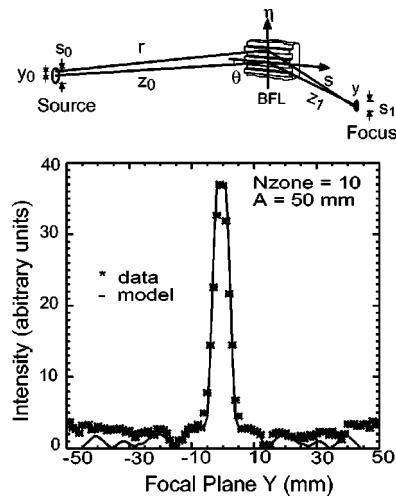

FIG. 3. The coordinate system used for the BFL model described in Eq. (1) (top graph). The bottom graph shows background subtracted experimental data(*) against a model calculation based on Eq. (1) (line).

coherence of the source, which can be estimated using $\lambda L/\delta$, where $\delta (=150 \, \mu m)$ is the source size and $L(=60 \, m)$ is the distance from the source to the optic, is approximately 40 μm. This coherent length is smaller than the aperture of the BFL used (260 μm). Based on demagnification of the source, the expected focal spot size of a BFL with a 0.6 m focal length is ~1.5 μm, which is larger than the intrinsic diffraction-limited spatial resolution (~0.25 μm) for the BFL used in the experiment.

The focal plane intensity distribution for the test BFL was measured by scanning a 5-μm-wide Ni strip through the beam and recording the Ni K-shell fluorescence (7.47 keV) with an energy dispersive Ge detector. This energy discriminative method minimizes background noise due the scattering of the incident radiation because of the wide energy separation between the fluorescent and incident x rays. The Ni strip (~1000 Å thick) was deposited on a (100) Si wafer by e-beam evaporation on a photoresist mask patterned using e-beam lithography. The well-controlled width and edge sharpness of the strip provides a well defined resolution function for deconvolution of the experimental data. Figure 2 (bottom) shows the first order focal plane diffraction pattern in the vertical direction produced by a sagittally focusing 0.2 μm linewidth 280 zone GaAs linear BFL at 12 keV. The pattern consists of a central sharp peak (focus) as well as higher order fringes riding on top of a plateau formed by the unfocused (zeroth order) beam and defocused higher order peaks.[11] The two peaks at both edges of the beam are due to Fresnel diffraction by the two aperture-defining slits.[12]

The focusing data shown in Fig. 2 can be directly compared to various theoretical models of the BFL. Because of the intense computational requirements, the dynamical diffraction models are of limited use when iterative simulation is needed in the design optimization process.[7–9] Some kinematic models have been proposed, but have not been verified directly with experimental data.[5,13]

To develop a simple model which can be used to predict the diffractive properties of BFLs, we treat these lenses simply as optical phase zone plate with intensity modulated by the reflectivity of the crystal. The thickness difference (zone height) between adjacent zones can be modeled as having the effect of retarding the phase of the waves coming from the

top zones by $\varphi = 4\pi\delta h/\lambda \sin\theta$, where $n = 1 - \delta$ is the index of refraction of the substrate material, h the zone depth and θ the Bragg angle.[1] We assume that the beam is uniform along the length of the BFL (no in plane focusing). The partially coherent source is divided in a small coherent sections with a Gaussian intensity profile and the intensities (rather than amplitudes) from these segments are integrated. Using a coordinate system as shown in Fig. 3 (top) the vertical focal plane intensity distribution can be written as a simplified Fresnel integral

$$I(y) \propto \int_{-s_0/2}^{s_0/2} e^{-y_0^2/2\sigma^2} dy_0$$

$$\times \left| -\frac{ik}{4\pi} |F_{hkl}| \sum_{-N_{zone}}^{N_{zone}} e^{i\varphi_n} \int_{rs_n}^{r_{n+1}} \frac{e^{ik(r+s)}}{rs} d\eta \right|^2, \quad (1)$$

where

$$r = \sqrt{z_0^2 + (\eta - y_0)^2}, \quad s = \sqrt{z_1^2 + (\eta - y)^2}$$

are the optical path functions, s_0 the source size, $|F_{hkl}|$ the Bragg amplitude of the substrate, and $\phi_n = 0$ for even numbered zones and $\phi_n = 4\pi\delta h/\lambda \sin\theta$ (=0.78π for a 0.53-μm-thick GaAs layer at 12 keV) for odd numbered zones. Using the first order term of Taylor's expansion of the integral inside the summation, one arrives at an approximate analytical form of Error function for the focus, as opposed to Bessel functions for circular zone plates.[11]

Figure 3 (bottom) shows a computer calculation, based on Eq. (1) using a bivariate Gaussian numerical integration method, of the focusing pattern of a 10 zone linear BFL versus the experimental data. The calculation was done using experimental parameters without iterative fitting. The calculated diffraction pattern was then convolved with a 5-μm-wide sampling function and scaled to superimpose on the experimental data. The model calculation correctly reproduced the central focus as well as the key features in the secondary fringes. Calculations using number of zones larger or smaller than 10 did not match the experimental data well, the deviations being most evident at the first minimum position. In the experiment, a BFL with 10 zones has a device

Appl. Phys. Lett., Vol. 77, No. 3, 17 July 2000

Li *et al.* 315

aperture of approximately 50 μm, which is close to the source transverse coherence of ~40 μm at the device. In other words, out of the illuminated 280 zones in the BFL, only the central 10 zones contributed to focusing due to the fact that the source is only partially coherent. *Thus the source transverse coherence size defines an effective device aperture for focusing*. Based on model calculation the full width at half maximum focus size is ~1.8 μm, which is larger than the expected focus size of 1.5 μm based on geometric demagnification. This focus broadening is most likely the result of having only finite number of zones contributing to focusing. For optimal focusing the BFL should be designed to match the coherence property of the source, which can be carried out using the computationally efficient linear BFL model described above. These x-ray linear microprobes are currently been used in structural studies using x-ray microdiffraction on filamental protein assemblies and complex fluids in confinement using the newly developed x-ray surface forces apparatus and patterned substrates.[14,15]

[1] V. V. Aristov, Y. A. Basov, T. E. Goureev, A. A. Snigirev, T. Ishikawa, K. Izumi, and S. Kikuta, Jpn. J. Appl. Phys., Part 1 **31**, 2616 (1992).

[2] A. Snigirev, I. Snigireva, P. Bosecke, S. Lequien, and I. Schelokov, Opt. Commun. **135**, 378 (1997).

[3] B. Lai *et al.*, Rev. Sci. Instrum. **66**, 2287 (1995).

[4] W. B. Yun, P. J. Viccaro, B. Lai, and J. Chrzas, Rev. Sci. Instrum. **63**, 582 (1992).

[5] A. Snigirev, Rev. Sci. Instrum. **66**, 2053 (1995).

[6] Y. Li, G. C. L. Wong, C. R. Safinya, E. Caine, E. L. Hu, D. Haeffner, P. Fernandez, and W. Yun, Rev. Sci. Instrum. **66**, 2844 (1998).

[7] A. Mirone, M. Idir, P. Dhez, G. Soullie, and A. Erko, Opt. Commun. **111**, 191 (1994).

[8] Z. Le and J. C. Shoufou Pan, Opt. Commun. **149**, 223 (1998).

[9] F. Montiel and M. Neviere, J. Opt. Soc. Am. A **12**, 2672 (1995).

[10] E. J. Caine, S. Shi, E. L. Hu, Y. Li, S. H. J. Idziak, G. Subramanian, and C. R. Safinya, Microelectron. Eng. **35**, 289 (1997).

[11] A. G. Michette, *Optical Systems for Soft X Rays* (Plenum, New York, 1986).

[12] G. R. Fowles, *Introduction to Modern Optics*, 2nd ed. (Dover, New York, 1989).

[13] F. N. Chukhovskii, W. Z. Chang, and E. Forster, Opt. Commun. **124**, 23 (1996).

[14] G. C. L. Wong, Y. Li, I. Koltover, C. R. Safinya, Z. Cai, and W. Yun, Appl. Phys. Lett. **73**, 2042 (1998).

[15] S. H. J. Idziak *et al.*, Science **V264**, 1915 (1994).